

A Deep Learning Method for ECG Signal Prediction Based on VMD, Cao Method, and LSTM Neural Network

Fuying Huang (✉ h_f_y2002@163.com)

South China University of Technology <https://orcid.org/0000-0003-1422-2571>

Tuanfa Qin

Guangxi University

Limei Wang

Guangxi Meteorological Information Center

Haibin Wan

Guangxi University

Research

Keywords: deep learning, prediction accuracy, ECG, VMD, Cao method, LSTM neural network

Posted Date: January 7th, 2021

DOI: <https://doi.org/10.21203/rs.3.rs-139350/v1>

License:  This work is licensed under a Creative Commons Attribution 4.0 International License.

[Read Full License](#)

A deep learning method for ECG signal prediction based on VMD, Cao method, and LSTM neural network

Fuying Huang^{1*}, Tuanfa Qin², Limei Wang³ and Haibin Wan²

* Correspondence: h_f_y2002@163.com

¹ School of Electronic and Information, South China University of Technology, Guangzhou 510641, China

Full list of author information is available at the end of the article

Abstract

Background: In body area network (BAN), accurate prediction of ECG signal can not only let doctors know the patient's condition in advance, but also help to reduce the energy consumption of sensors. In order to improve the accuracy of ECG signal prediction, this paper proposes a deep learning method for ECG signal prediction.

Methods: The proposed prediction method combines variational mode decomposition (VMD), Cao method and a long short-term memory (LSTM) neural network. In the method, VMD decomposes ECG data into a series of intrinsic mode functions (IMFs), which reduces the non-stationary character of ECG signals and helps to improve the prediction accuracy. Cao method is used to determine the input dimension of LSTM input layer, namely, the minimum embedding dimension of each IMF is the input dimension of LSTM input layer. Each IMF is predicted by a LSTM neural network which adopts Adam optimizer. All IMFs predictions are aggregated to get the final prediction result.

Results: To evaluate the prediction accuracy of the proposed method, simulation experiments are carried out on ECG data from the MIT-BIH Arrhythmia Database. Experimental results show that the RMSE (root mean square error) and MAE (mean absolute error) of the proposed model are 0.001326 and 0.001044 respectively, which are more than 10 percent lower than the traditional prediction methods.

Conclusions: Compared with some traditional prediction methods, the proposed prediction method improves the prediction accuracy obviously.

Keywords: deep learning; prediction accuracy; ECG; VMD; Cao method; LSTM neural network

Introduction

ECG is one of the most commonly used methods in clinic. It is significant for doctors and BAN to predict ECG signal accurately. On the one hand, doctors can know the patient's condition in advance; on the other hand, it helps sensors in BAN to reduce energy consumption. In BAN, there are some sensors placed under the skin or inside the body, and their batteries are inconvenient to replace. Therefore, it is necessary to reduce energy consumption and prolonging the lifetime of a sensor. If a prediction model is established in both sensor node and sink node, when the prediction error exceeds the specified threshold value, the sensor node will send the measured data,

otherwise, it will not send the measured data [1]. According to this view, the prediction technology can reduce data transmission and reduce the energy consumption of a sensor. In BAN, the data volume of the ECG signal is the largest, which is several times higher than that of other signals. The accurate prediction of an ECG signal can eliminate the need to collect data in real time and reduce the amount of data transmission, so as to achieve the purpose of reducing the energy consumption of a sensor.

In BAN, the data collected by sensors are time series data. For time series prediction, prediction model is the key factor of prediction accuracy. With the application of deep learning more and more widely, many scholars began to use deep learning technology to study time series prediction. As a typical deep learning model, Recurrent neural network(RNN) has been applied in time series prediction [2-4]. Compared with the traditional time series prediction methods, RNN improves the prediction accuracy, but it still has the shortcomings of gradient disappearance and gradient explosion. LSTM is an improved RNN, which overcomes the shortcomings of RNN. At present, LSTM has achieved wide application in natural language processing [5-6], machine translation [7-8], and handwriting recognition [9]. Many researchers are focused on the time series prediction with LSTM. Essien et al. [10] proposed a deep ConvLSTM autoencoder (2-DConvLSTMAE) predictive model for machine speed prediction. The predictive model was applied to the multistep time-series prediction problem and achieved improved predictive performance. Du et al.[11] proposed a deep irregular convolutional residual LSTM model for predicting the flows of crowds in transportation lines. The proposed model outperforms both traditional and deep learning based urban traffic passenger flow prediction methods. Wang et al. [12] proposed an earthquake prediction system. The proposed system can make accurate predictions with different temporal and spatial prediction granularities. Some literatures proposed to use VMD combined with LSTM to predict time series [13-14], but they seldom discussed how to solve the input length problem of LSTM input layer. Relevant literature shows that LSTM is indeed more effective than the traditional RNN model in the analysis and prediction of time series data [15-16].

This paper focuses on the prediction of an ECG signal. Because an ECG signal is a nonlinear and non-stationary time series signal with an inherent random feature, it is difficult to predict accurately. At present, there are some literatures on the prediction of ECG signals. Wei *et al.* [17] developed a universal model for highly accurate prediction of ECGs and EEGs. The model combined a convolutional neural network (CNN) and bi-directional recurrent neural network (BRNN). Sun *et al.* [18] proposed a prediction method of an ECG signal using an error backpropagation neural network (BPNN) and VMD. An ECG signal prediction method based on phase space reconstruction (PSR) and BPNN was proposed in [19], with accuracy close to that of the previously mentioned method. An ECG signal prediction method based on autoregressive integrated moving average (ARIMA) model and discrete wavelet transform (DWT) was proposed in [20]. Although the prediction accuracy of the method is relatively high, it needs to smooth the ECG signal in advance, and there is a certain signal distortion. In [21], an ECG signal prediction method was proposed. In

the method, the PSR and the TS fuzzy model were used to predict an ECG signal. The prediction error of the method was the same order of magnitude as that in [18] and [19].

The prediction accuracy of the existing ECG prediction methods is relatively low. To improve the prediction accuracy of ECG signal, we propose a deep learning method for ECG signal prediction using VMD, Cao method, and LSTM neural network. Firstly, we use VMD to preprocess ECG data. VMD decomposes a non-stationary ECG into some stationary IMFs, which is helpful to improve the prediction accuracy. Secondly, the optimal input dimension of LSTM input layer is determined by Cao method. Finally, we use the Adam optimizer to optimize the parameters of LSTM and predict ECG signal by the LSTM. The rest of this paper is organized as follows. Results section describes a simulation experiment and the analysis of its results. Discussion section compares the proposed prediction method with some competitive prediction methods. Conclusions section provides concluding remarks. Methods section describes in detail an ECG signal prediction method based on VMD, Cao method, and LSTM neural network.

Results

All ECG data in the simulation experiment are from the MIT-BIH Arrhythmia Database [22]. We selected No.100 ECG data, which consists of 2,768 data points, for the experiment. We used two-thirds of No.100 ECG data as the training set (i.e., 1845 data points) and the remaining one-third as the test set (i.e., 923 data points). All experiments were carried out in MATLAB and Python compiling environment. The LSTM model was implemented in a Theano framework based on Keras deep learning tools. The parameters of LSTM are epochs=250, batch_size=4, optimizer=Adam, loss=mean_squared_error, and activation=Relu.

The common performance measures of prediction methods are RMSE, MAE, mean absolute percentage error (MAPE), and R-square (R^2), defined as

$$RMSE = \sqrt{\frac{1}{N} \sum_{n=1}^N (X(n) - \hat{X}(n))^2} \quad (1)$$

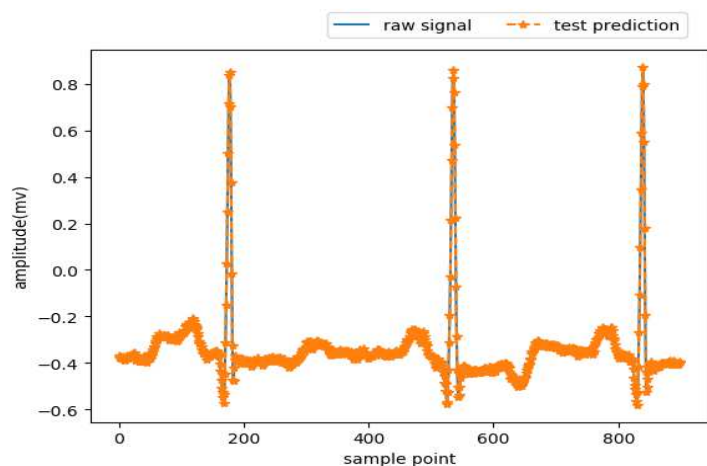
$$MAE = \frac{1}{N} \sum_{n=1}^N |X(n) - \hat{X}(n)| \quad (2)$$

$$MAPE = 100 \times \frac{1}{N} \sum_{n=1}^N \left| \frac{X(n) - \hat{X}(n)}{X(n)} \right| \quad (3)$$

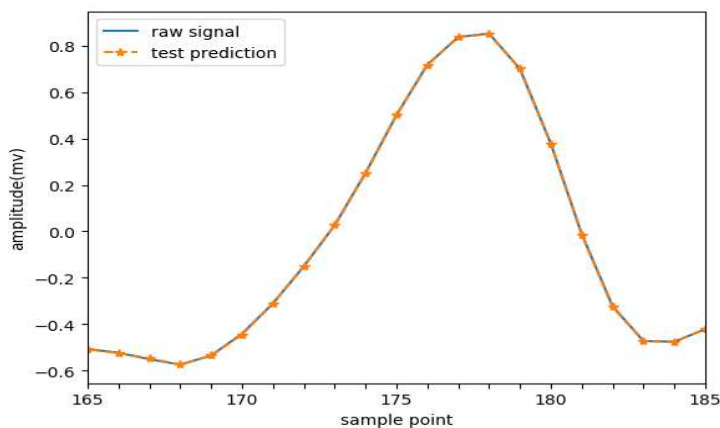
$$R^2 = 1 - \frac{\sum_{n=1}^N |X(n) - \hat{X}(n)|^2}{\sum_{n=1}^N |X(n) - X_{mean}|^2} \quad (4)$$

where $\hat{X}(n)$ is the predicted value of $X(n)$, N is the number of $X(n)$, and X_{mean} is the mean of $X(n)$.

The proposed method is used to predict the test set of No. 100 ECG, as shown in Figure 1.



(a)



(b)

Figure 1 Prediction result of the test set. (a) the prediction waveform; (b) the local amplification of (a), the amplification range is [165, 185].

In Figure 1, raw signal represents the original signal and test prediction represents the predicted signal. Figure 1 shows that the original ECG waveform is consistent with its predicted waveform. The prediction indexes of the test set are shown in Table 1.

Table 1 Prediction indexes of the test set of No.100 ECG

RMSE	MAE	MAPE	R ²
0.001326	0.001044	0.336560	0.999936

Table 1 shows that the prediction error is very small and the correlation between the predicted signal and the original signal is good.

Discussion

Compared with some prediction methods

We compared the proposed method with the prediction methods of references [18], [19], and [21]. We experimented on the same data source, No. 100 ECG, and the experimental results are shown in Table 2 and Figure 2.

Table 2 Comparison with some prediction methods

Methods	RMSE	MAE
This paper	0.001326	0.001044
Sun et al.[18]	0.0233	0.0157
Sun et al.[19]	0.0423	0.0240
Su et al.[21]	0.0146	0.0106

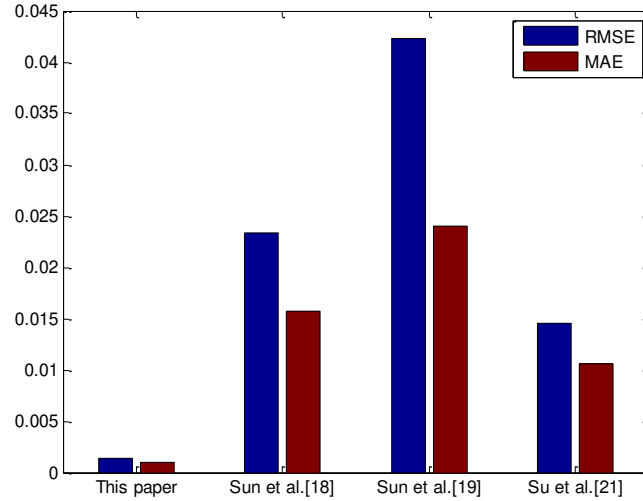


Figure 2 Comparison with some prediction methods

As shown in Table 2 and Figure 2, the RMSE and MAE of the proposed method are much smaller than those of references [18], [19] and [21]. This illustrates that the prediction accuracy of this paper is much higher than that of references [18], [19] and [21], respectively.

Compared with some hybrid prediction methods

In addition, the proposed method (VMD-Cao-LSTM) was compared with other traditional hybrid methods, such as the method based on wavelet transform(WT), PSR, and radial basis function(RBF) neural network (WT-PSR-RBF); the method based on empirical mode decomposition (EMD), PSR, and RBF neural network (EMD-PSR-RBF); the method based on VMD, PSR, and BP neural network (VMD-PSR-BP); and the method based on VMD, generalized regression neural network (GRNN) , and PSR (VMD-PSR-GRNN). The experimental data were No.

100 ECG. The trained set has 1845 data points and the test set has 923 data points. The experimental results were shown in Table 3.

Table 3 Prediction results of different methods

Prediction methods	RMSE	MSE	MAE
VMD-Cao-LSTM	0.001326	2.0e-06	0.001044
WT-PSR-RBF	0.0033	1.0850e-05	0.0020
EMD-PSR-RBF	0.0131	1.7096e-04	0.0093
VMD-PSR-BP	0.0174	3.0434e-04	0.0115
VMD-PSR-GRNN	0.0126	1.5944e-04	0.0087

It is obvious from Table 3 that the prediction performance of this paper (VMD-Cao-LSTM) is better than that of WT-PSR-RBF, EMD-PSR-RBF, VMD-PSR-BP and VMD-PSR-GRNN.

Compared with some deep learning prediction methods

We also compared the proposed method with some deep learning prediction methods. The comparison results were shown in Table 4 and Figure 3.

Table 4 Comparison with some deep learning prediction methods

Prediction methods	RMSE	MAE
VMD-Cao-LSTM	0.001326	0.001044
LSTM	0.014773	0.011094
MLP	0.012900	0.009502
CNN	0.026436	0.018289

Table 4 shows that the RMSE and MAE of VMD-Cao-LSTM are obvious less than those of LSTM, MLP and CNN.

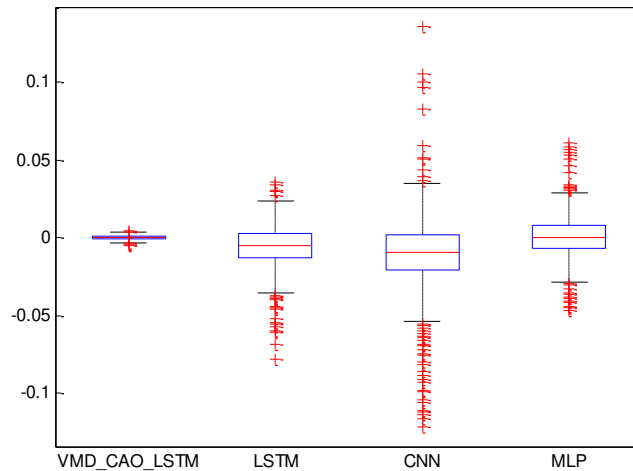


Figure 3 The box plot of prediction errors

In Figure 3, the prediction error of VMD-Cao-LSTM is less than that of LSTM, CNN and multi-layer perceptron (MLP). Table 4 and Figure 3 show that the prediction performance of VMD-Cao-LSTM outperforms that of LSTM, CNN and MLP.

Conclusions

In this paper, we review the latest development of ECG prediction methods. Based on the analysis of VMD, Cao method and LSTM, we propose a deep learning method for ECG signal prediction. Using the ECG data of the MIT-BIH Arrhythmia Database as the data source, we evaluate the prediction performance of the proposed method. Simulation results show that the RMSE and MAE of the proposed prediction method are only 10^{-3} orders of magnitude, while those of the general prediction methods are 10^{-2} orders of magnitude. We draw a conclusion that the prediction method proposed in this paper significantly improves the accuracy of ECG signal prediction. In the next work, we will study how to use the prediction method proposed in this paper to reduce the energy consumption of the sensor.

Methods

VMD

Variational mode decomposition (VMD) decomposes an input signal into a series of discrete band-limited IMFs around the center frequency. In time series prediction, the function of VMD is to reduce the non-stationary character of time series, which is helpful to improve the accuracy of prediction. Each IMF component is obtained through the following three steps:

Step 1: Calculate the analytic signal of each modal function $u_k(t)$ by Hilbert transform

$$(\delta(t) + \frac{j}{\pi t}) * u_k(t) \quad (5)$$

Step 2: Multiply the analytical signal by the estimated center frequency $e^{-jw_k t}$, and move it to the base frequency spectrum, which is

$$[(\delta(t) + \frac{j}{\pi t}) * u_k(t)] e^{-jw_k t} \quad (6)$$

Step 3: Estimate the bandwidth of each mode by Gaussian smoothing of the demodulated signal, i.e., the L^2 norm of the gradient. The constrained variational model is

$$\begin{cases} \min_{\{u_k\}, \{w_k\}} \left\{ \sum_k \left\| \partial t [(\delta(t) + \frac{j}{\pi t}) * u_k(t)] e^{-jw_k t} \right\|_2^2 \right\} \\ s.t. \sum_k u_k = x \end{cases} \quad (7)$$

where x is the input signal and $\|g\|_2$ is the Euclidian distance. In order to find the

optimal solution of the above problem, turn the constrained variational model into an unconstrained variational model by introducing the quadratic penalty factor α and Lagrange multiplication operator $\lambda(t)$. The extended Lagrange expression is

$$L(\{u_k\}, \{w_k\}, \lambda(t)) = \alpha \sum_k \left\| \partial_t \left[\left(\delta(t) + \frac{j}{\pi t} \right) * u_k(t) \right] e^{-jw_k t} \right\|_2^2 + \left\| x - \sum_k u_k \right\|_2^2 + \langle \lambda(t), x - \sum_k u_k \rangle \quad (8)$$

Find the saddle point of the extended Lagrange expression using the alternating direction multiplier method (ADMM) [23] to solve the extended Lagrange problem.

The saddle point is obtained by alternating renewal $u_k^{n+1}, w_k^{n+1}, \lambda^{n+1}$. The specific implementation process of VMD is as follows:

Step 1: Initialize $\{u_k^1\}, \{w_k^1\}, \lambda^1$, and set $n = 0$.

Step 2: Update u_k^{n+1}, w_k^{n+1} , and λ^{n+1} . The formulas for these are

$$u_k^{n+1}(w) = \frac{\hat{x}(w) - \sum_{i < k} u_i^{n+1}(w) - \sum_{i > k} u_i^n(w) + \lambda^n(w) / 2}{1 + 2\alpha(w - w_k^n)^2} \quad (9)$$

$$w_k^{n+1} = \frac{\int_0^\infty w |u_k^{n+1}(w)|^2 dw}{\int_0^\infty |u_k^{n+1}(w)|^2 dw} \quad (10)$$

$$\lambda^{n+1}(w) = \lambda^n(w) + \tau \left(\hat{x}(w) - \sum_k |u_k^{n+1}(w)| \right) \quad (11)$$

where $u_k^{n+1}(w)$, $\lambda^n(w)$, and $\hat{x}(w)$ are the Fourier transforms of the signals $u_k^{n+1}(t)$, $\lambda(t)$, and $x(t)$, respectively. τ is the step update coefficient.

Step 3: Repeat step 2 until the convergence condition is reached

$$\sum_k \left\| u_k^{n+1} - u_k^n \right\|_2^2 / \left\| u_k^n \right\|_2^2 < \varepsilon \quad (12)$$

where ε is a judgment threshold.

Before VMD, the number K of IMFs needs to be predetermined. K can be selected according to the ratio of residual energy R_{res} to the original signal energy. The R_{res} is defined as follows:

$$R_{res} = \frac{1}{N} \sum_{n=1}^N \left| \frac{X(n) - \sum_{k=1}^K u_k(n)}{X(n)} \right| \quad (13)$$

where $X(n)$ is the original signal, $u_k(n)$ is the IMF, and N is the sample number. When R_{res} is less than 1% and there is no significant downward trend, the number K can be determined [24]. For the No. 100 ECG data, the R_{res} of VMD with different K are

shown in Table 5.

Table 5 The R_{res} of VMD with different K

K	1	2	3	4	5	6	7	8	9	10
R_{res}	0.0658	0.0258	0.0116	0.0064	0.0035	0.0021	0.0018	0.0015	0.0018	0.0017
K	11	12	13	14	15	16	17	18	19	20
R_{res}	0.0017	0.0015	0.0016	0.0012	0.0012	0.0011	0.0011	0.0012	0.0012	0.0010

Table 5 shows that the R_{res} has no obvious downward trend when $K = 14$. Therefore, we set $K = 14$ in the experiment.

Cao method

Cao method was proposed to determine the minimum embedding dimension of a time series by Cao [25]. In Cao method, the time-delay parameter τ is necessary before the minimum embedding dimension is determined. For a time series x_1, x_2, \dots, x_N , the time-delay vectors can be reconstructed as follows:

$$y_i(m) = (x_i, x_{i+\tau}, \dots, x_{i+(m-1)\tau}), \quad i = 1, 2, \dots, N - (m-1)\tau \quad (14)$$

Cao method is described as follows:

$$E(m) = \frac{1}{N - m\tau} \sum_{i=1}^{N-m\tau} \frac{\|y_i(m+1) - y_{n(i,m)}(m+1)\|}{\|y_i(m) - y_{n(i,m)}(m)\|} \quad (15)$$

$$E1(m) = \frac{E(m+1)}{E(m)} \quad (16)$$

where m is the embedding dimension, τ is the time delay, $y_i(m)$ is the i th reconstructed vector with embedding dimension m , $\|\cdot\|$ is Euclidian distance, $n(i, m)$ ($1 \leq n(i, m) \leq N - m\tau$) is an integer which $y_{n(i,m)}(m)$ is the nearest neighbour of $y_i(m)$. If $E1(m)$ stops changing when m is greater than the value m_0 , m_0+1 is the minimum embedding dimension. After VMD of No.100 ECG data, we set $\tau = 1$ and obtain the minimum embedding dimensions m of each IMF, as shown in Table 6.

Table 6 The embedding dimension of each IMF

IMF	1	2	3	4	5	6	7	8	9	10	11	12	13	14
m	6	6	6	6	7	6	6	7	10	7	7	8	8	12

The minimum embedding dimension m is the input dimension of LSTM neural network.

LSTM neural network

As one of the classic models of deep learning, LSTM is widely used in time series prediction. LSTM is an improved RNN model, which solves the problems of gradient disappearance and gradient explosion that RNN cannot overcome. Each LSTM unit is composed of a memory cell and three gates: an input gate, a forget gate, and an output gate. The functions of these three gates are: the input gate decides the information that should be input; the forget gate determines the information that should be discarded; the output gate decides the information that should be output. The architecture of LSTM unit is shown in Figure 4.

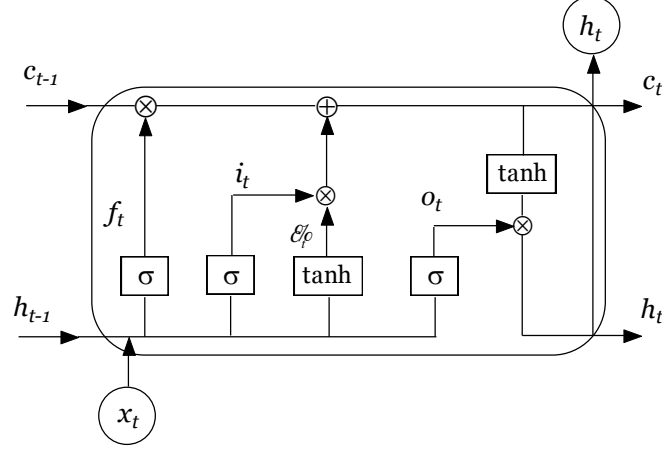


Figure 4 The architecture of LSTM unit

The output values of three gates (input gate i_t , forget gate f_t and output gate o_t) and updated information are expressed in the following formulas:

$$f_t = \sigma(W_f[h_{t-1}, x_t] + b_f) \quad (17)$$

$$i_t = \sigma(W_i[h_{t-1}, x_t] + b_i) \quad (18)$$

$$o_t = \sigma(W_o[h_{t-1}, x_t] + b_o) \quad (19)$$

$$\mathcal{E}_t = \tanh(W_c[h_{t-1}, x_t] + b_c) \quad (20)$$

$$c_t = f_t * c_{t-1} + i_t * \mathcal{E}_t \quad (21)$$

$$h_t = o_t * \tanh(c_t) \quad (22)$$

where W and b denotes weight matrices and bias vectors of gates, respectively. In addition, σ and \tanh are the activation functions between different layers, c_t is the current state of the cell, \mathcal{E}_t is the unit state of the current input, and h_t is the current output of the cell. The expressions of σ and \tanh are as follows:

$$\sigma(x) = \frac{1}{1 + e^{-x}} \quad (23)$$

$$\tanh(x) = \frac{\sinh(x)}{\cosh(x)} = \frac{e^x - e^{-x}}{e^x + e^{-x}} = 2\sigma(2x) - 1 \quad (24)$$

By introducing cell state c_t and three gate structures of forgetting gate, input gate and output gate, LSTM has the ability of long-term and short-term memory, thus solving the problems of gradient disappearance and gradient explosion of RNN. Compared with other neural networks, LSTM is more suitable for time series data prediction.

The proposed prediction method for ECG signal

Based on the study of ECG signal prediction, this paper proposes a hybrid method of ECG signal prediction. Its flowchart is shown in Figure 5.

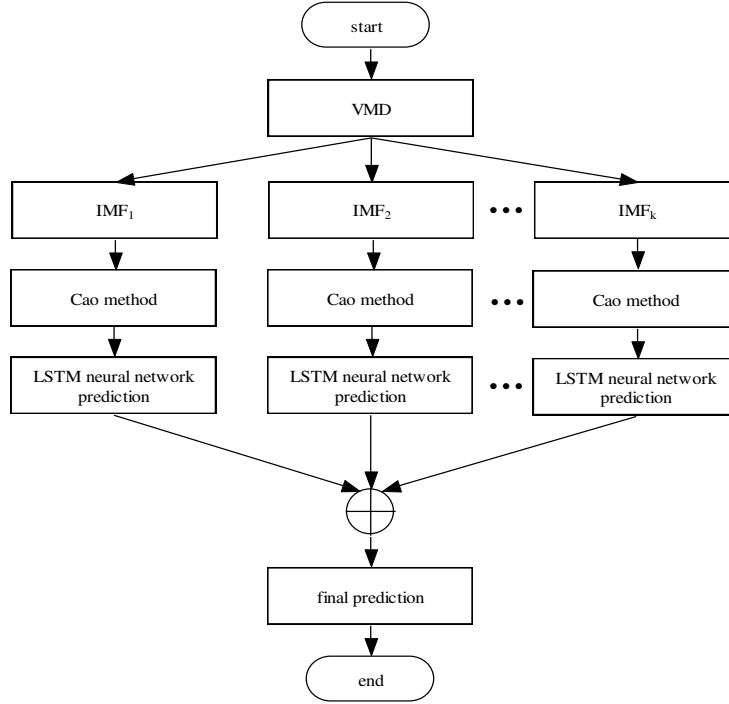


Figure 5 Flowchart of the proposed method

The prediction steps of the proposed method are as follows:

Step 1: Decompose ECG data into K IMFs by VMD. In the experiment, we use $K = 14$ to get a better prediction result.

Step 2: Determine the input variables of the LSTM neural network by Cao method.

Step 3: Establish a LSTM neural network and use it to predict the test set of each IMF.

Step 4: Add the prediction results of the LSTM neural network to obtain the final ECG signal prediction result.

Step 5: Analyze the prediction error and compare it to other prediction methods.

Abbreviations

BAN: body area network; VMD: variational mode decomposition; IMFs: intrinsic mode functions; LSTM: long short-term memory; RNN: recurrent neural network; CNN: convolutional neural network; BRNN: bi-directional recurrent neural network; BPNN: backpropagation neural network; DWT: discrete wavelet transform; PSR: phase space reconstruction; ARIMA: autoregressive integrated moving average; RMSE: root mean square error; MAE: mean absolute error; MAPE: mean absolute percentage error; WT: wavelet transform; EMD: empirical mode decomposition; RBF: radial basis function; GRNN: generalized regression neural network; MLP: multi-layer perceptron; ADMM: alternating direction multiplier method.

Acknowledgements

This work was supported by Guangxi Key Laboratory of Multimedia Communications and Network Technology, and the high-performance computing platform of Guangxi University.

Author Contributions

Conceptualization, F.H. and L.W.; methodology, F.H.; software, F.H. and L.W.; validation, L.W. and H.W.; formal analysis, L.W.; investigation, F.H. and T.Q.; resources, H.W.; data curation, F.H. and T.Q.; writing—original draft preparation, F.H.; writing—review and editing, F.H., L.W. and T.Q.; visualization, L.W.; supervision, T.Q.; project administration, T.Q. and H.W.; funding acquisition, T.Q. and H.W.

Ethics approval and consent to participate

Not applicable

Consent for publication

Not applicable

Funding

This work is supported by National Natural Science Foundation of China (Nos. 61761007 and 61661005).

Availability of data and materials

In this paper, All ECG data are from MIT-BIH Arrhythmia Database. MIT-BIH Arrhythmia Database is available online: <https://www.physionet.org/content/mitdb/1.0.0/>

Competing interests

The authors declare that they have no competing interests.

Author details

¹ School of Electronic and Information Engineering, South China University of Technology, Guangzhou 510641, China.

² School of Computer, Electronics and Information, Guangxi University, Nanning 530004, China.

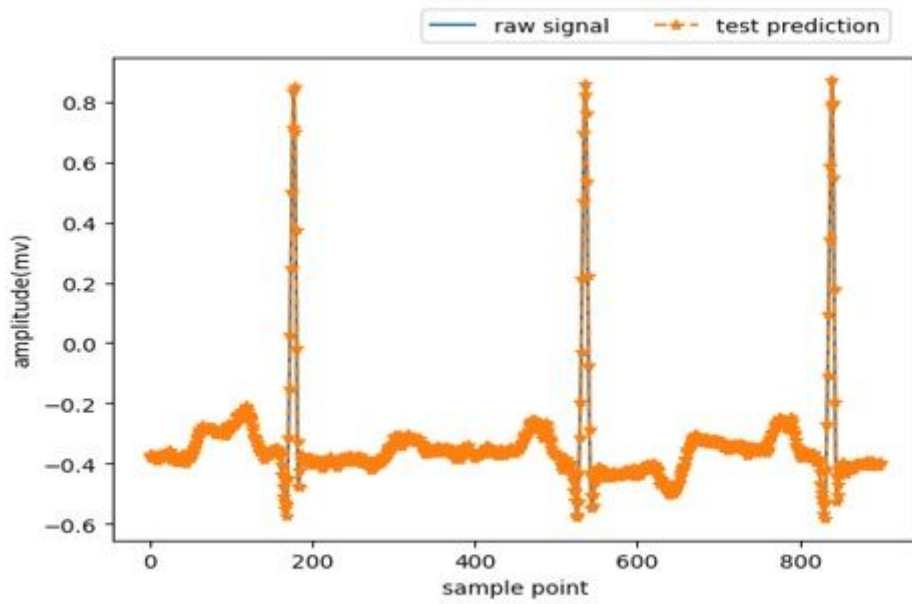
³ Guangxi Meteorological Information Centre, Nanning 530022, China.

References

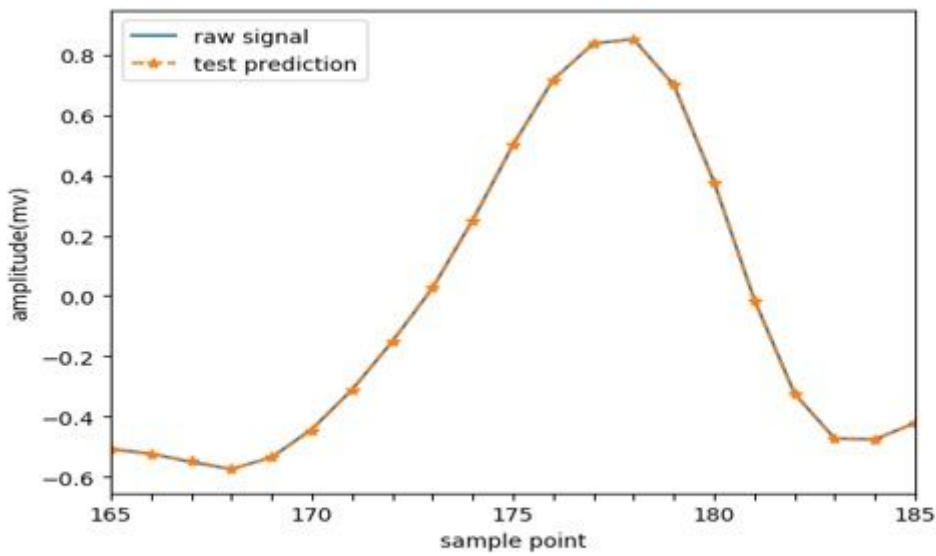
1. Yu LN. The research on green data fusion model and transmission scheduling algorithm of wireless Body Area Networks. Ph.D. dissertation, China Agricultural University, Beijing, China, 2016.
2. Shahtalebi S, Atashzar SF, Patel RV, Mohammadi A. HMFP-DBRNN: Real-Time Hand Motion Filtering and Prediction via Deep Bidirectional RNN. *IEEE Robotics and Automation Letters*. 2019; 4(2): 1061-1068.
3. Sha S, et al. RNN-Based Subway Passenger Flow Rolling Prediction. *IEEE Access*. 2020; 8:15232-15240.
4. Liu W, Shoji Y. DeepVM: RNN-Based Vehicle Mobility Prediction to Support Intelligent Vehicle Applications. *IEEE Transactions on Industrial Informatics*. 2020; 16(6): 3997-4006.
5. Wu Y, et al. Google's Neural Machine Translation System: Bridging the Gap between Human and Machine Translation. 2016.
6. Sundermeyer M, et al. From feedforward to recurrent lstm neural networks for language modeling. *IEEE Transactions on Audio, Speech, and Language Processing*. 2015; 23(3):517-529.
7. Kim M, et al. Speaker-Independent silent speech recognition from flesh-point articulatory movements using an LSTM neural network. *IEEE/ACM Trans. Audio network. IEEE/ACM Trans. Audio Speech Lang. Process*. 2017; 25 (12): 2323–2336.
8. Sutskever I, Vinyals O, Le QV. Sequence to Sequence Learning with Neural Networks. *Advances in Neural Information Processing Systems*. 2014; 4: 3104-3112.
9. Zhang XY, et al. End-to-End online writer identification with recurrent neural network. *IEEE Trans. Human-Mach. Syst*. 2017; 47 (2): 285–292.
10. Essien A, Giannetti C. A Deep Learning Model for Smart Manufacturing Using Convolutional LSTM Neural Network Autoencoders. *IEEE Transactions on Industrial Informatics*. 2020;16(9): 6069-6078.
11. Du B, et al. Deep Irregular Convolutional Residual LSTM for Urban Traffic Passenger Flows Prediction. *IEEE Transactions on Intelligent Transportation Systems*. 2020; 21(3): 972-985.
12. Wang Q, Guo Y, Yu L, Li P. Earthquake Prediction Based on Spatio-Temporal Data Mining: An LSTM Network Approach. *IEEE Transactions on Emerging Topics in Computing*. 2020; 8(1): 148-158.
13. Han L, Zhang R, Wang X, Bao A, Jing H. Multi-step wind power forecast based on VMD-LSTM. *IET Renewable Power Generation*. 2019; 13(10): 1690-1700.
14. Sun Z, Zhao S, Zhang J. Short-Term Wind Power Forecasting on Multiple Scales Using VMD Decomposition, K-Means Clustering and LSTM Principal Computing. *IEEE Access*. 2019;7: 166917-166929.
15. Palangi H, Ward R, Deng L. Distributed Compressive Sensing: A Deep Learning Approach. *IEEE Transactions on Signal Processing*. 2016; 64(17): 4504–18.
16. Palangi H, et al. Deep Sentence Embedding Using Long Short-Term Memory Networks: Analysis and Application to Information Retrieval. *IEEE-ACM Trans Audio Speech Lang*. 2016;24(4):694–707.
17. Wei CX, Zhang C, Wu M. A study on the universal method of EEG and ECG prediction. 10th International Congress on Image and Signal Processing, BioMedical Engineering and Informatics (CISP-BMEI), Shanghai, China. 2017; 1-5.
18. Sun ZG, et al. An ECG signal analysis and prediction method combined with VMD and neural network. 7th IEEE International Conference on Electronics Information and Emergency Communication (ICEIEC), Macau. 2017;199-202.
19. Sun ZG, et al. Data Prediction of ECG Based on Phase Space Reconstruction and Neural Network. In *Proceedings of 2018 8th International Conference on Electronics Information and Emergency Communication (ICEIEC)*, Beijing, China. 2018; 162-165.

20. Huang FY, Qin TF, Wang LM, Wan HB, Ren JY. An ECG Signal Prediction Method Based on ARIMA Model and DWT. IEEE 4th Advanced Information Technology, Electronic and Automation Control Conference (IAEAC), Chengdu, China. 2019; 1298-1304.
21. Su F, Dong HS. Prediction of ECG Signal Based on TS Fuzzy Model of Phase Space Reconstruction. 12th International Congress on Image and Signal Processing, BioMedical Engineering and Informatics (CISP-BMEI), Suzhou, China. 2019; 1-6.
22. MIT-BIH Arrhythmia Database. Available online: <https://www.physionet.org/content/mitdb/1.0.0/>
23. Tosserams S, Etman LFP, Papalambros PY. An augmented Lagrangian relaxation for analytical target cascading using the alternating direction method of multipliers. Structural and Multidisciplinary Optimization. 2006; 31(3): 176-189.
24. Liu YS, Yang CH, Keke, Gui WH. Non-ferrous metals price forecasting based on variational mode decomposition and LSTM network. Knowledge-Based Systems. 2019;188:105006.
25. Cao L. Practical method for determining the minimum embedding dimension of a scalar time series. Physica D Nonlinear Phenomena. 1997; 110(1-2):43-50.

Figures



(a)



(b)

Figure 1

Prediction result of the test set. (a) the prediction waveform; (b) the local amplification of (a), the amplification range is [165, 185].

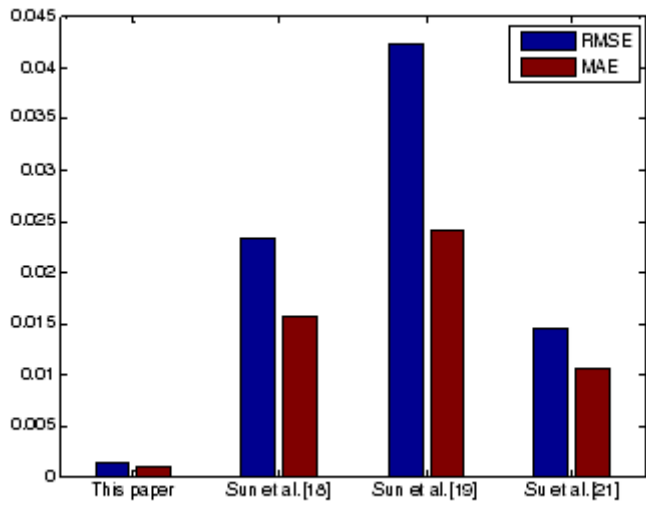


Figure 2

Comparison with some prediction methods

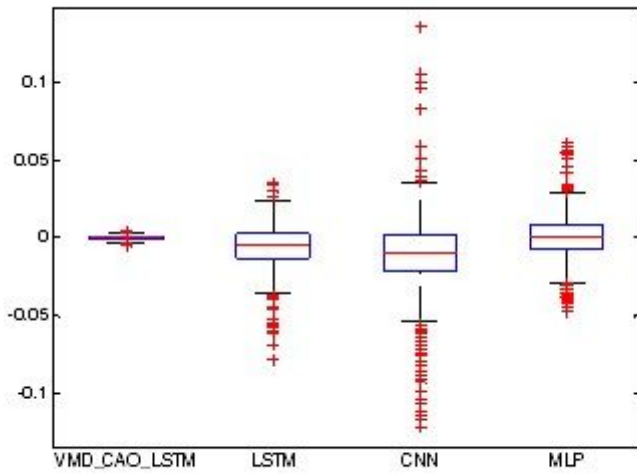


Figure 3

The box plot of prediction errors

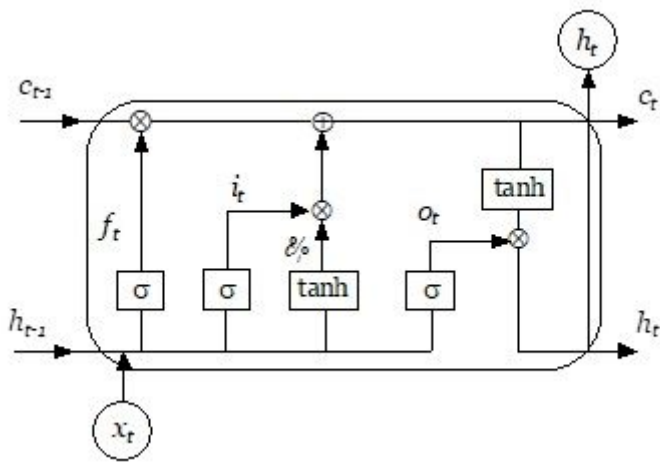


Figure 4

The architecture of LSTM unit

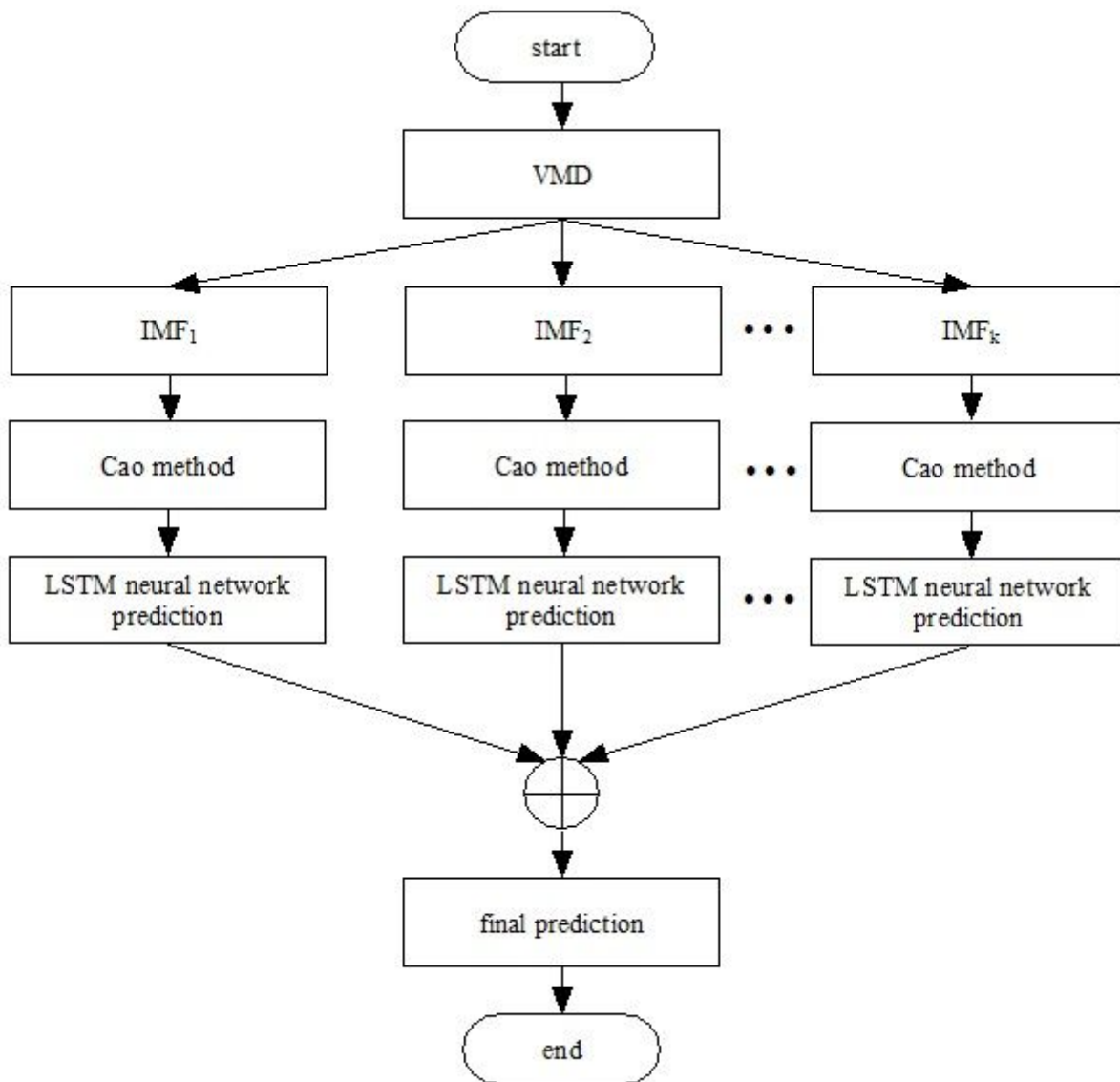


Figure 5

Flowchart of the proposed method